Fluctuation pressure of a fluid membrane between walls through six loops

Boris Kastening*

Institut für Materialwissenschaft, Technische Universität Darmstadt, Petersenstraße 23, D-64287 Darmstadt, Germany
and Institut für Theoretische Physik, Freie Universität Berlin, Arnimallee 14, D-14195 Berlin, Germany

The fluctuation pressure that an infinitely extended fluid membrane exerts on two enclosing parallel hard walls is computed. Variational perturbation theory is used to extract the hard-wall limit from a perturbative expansion through six loops obtained with a smooth wall potential. Our result $\alpha = 0.0821 \pm 0.0005$ for the constant conventionally parametrizing the pressure lies above earlier Monte Carlo results.

I. INTRODUCTION

Membranes are frequent structures in chemical and biological systems. Their dynamic behavior at finite temperature is of great interest, since their dominant repulsive force is given by thermal out-of-plane fluctuations [1,2]. If the temperature is sufficiently high, the details of the potential that inhibits their mutual penetration or that causes them to be confined to a certain geometrical region are unimportant. Then the membranes' thermal fluctuations may be described by a two-dimensional field theory with a hard-wall potential that describes their mutual interactions and the boundary conditions of the space accessible to them.

In an important class of membranes, their constituent molecules are able to move freely within them. The thermal fluctuations of these "fluid" membranes are controlled by their bending rigidity κ. The curvature energy of such a membrane is, in the harmonic approximation, described by

$$E = \frac{\kappa}{2} \int_A d^2x [\partial^2 \varphi(\boldsymbol{x})]^2, \qquad (1)$$

where the subscript refers to a plane with an area A that serves to parametrize the membranes' surface, and where $\varphi(\boldsymbol{x})$ describes the location of the membrane orthogonal to the point $\boldsymbol{x}$ on this plane. For the harmonic approximation to be valid, the membrane must not fluctuate too wildly and thus the temperature must also not be too high. It is difficult to describe the membranes' fluctuations outside the range of validity of the harmonic approximation, since then, e.g., overhangs with respect to any given plane and steric self-interactions of the membrane are possible.

There have been various theoretical approaches to compute the pressure of a single membrane between walls [1,3–8] or of a stack of membranes [1,3–5,9]. Here we consider a fluid membrane between two rigid walls and ask what pressure its classical statistical bending fluctuations exert on the walls. The plane parametrizing the membrane is taken to be midway between the enclosing walls, which are a distance d apart, and we consider the limit $A \to \infty$. By scaling analysis, the fluctuation pressure of the membrane has the form [1]

$$p = \alpha \frac{(k_B T)^2}{\kappa (d/2)^3}, \qquad (2)$$

and we are interested in the numerical value of α. Estimates of α range from crude theoretical estimates $\alpha \approx 0.0242$ by Helfrich [1] and $\alpha \approx 0.0625$ by Janke and Kleinert [3] (this reference also contains an early Monte Carlo result $\alpha = 0.060 \pm 0.003$) through Monte Carlo results

$$\alpha = 0.079 \pm 0.002 \qquad (3)$$

by Janke, Kleinert, and Meinhart [4] and

$$\alpha = 0.0798 \pm 0.0003 \qquad (4)$$

by Gompper and Kroll [5], and a theoretical estimate $\alpha \approx 0.0771$ by Kleinert [6] based on the analogy with a quantum mechanical particle in a box to a theoretical estimate $\alpha \approx 0.0797$ by Bachmann, Kleinert, and Pelster [7] using variational perturbation theory. Recently, we have extended the four-loop calculation in Ref. [7] to five loops [8] and found a value $\alpha \approx 0.0820$, outside the error bars of the Monte Carlo results. We were, however, unable to quote an error bar for our own result. In this work, we extend our computation through six loops. Together with improved resummation methods, this allows us to confirm the disagreement with the Monte Carlo results and put stringent error bars around our result.

Our work is structured as follows. In Sec. II, we briefly remind the reader how the hard walls may be modeled using an analytic potential and how a perturbative series for α may be derived. In Sec. III, the central results of the technically similar quantum mechanics (QM) problem of a particle in a box are listed since they are instrumental for extracting α for the membrane problem from its perturbative expansion in Sec. V. In Sec. IV, we directly resum the perturbative series for α. In Sec. V, we adjust the potential modeling the boundary conditions for the membrane problem so that the perturbative series for α of the QM problem is obtained. Appropriate resummation schemes let us then infer the distance of the walls described by the resulting potential, and this information is trivially translated into a value of α for the membrane problem. In Sec. VI, we summarize and briefly discuss our results.

―――――――
*Electronic address: kastening@oxide.tu-darmstadt.de

II. MODELING OF THE HARD WALLS

Consider a tensionless membrane between two large flat parallel walls of area A separated by a distance d, whose curvature energy is given by (1). The d-dependent part f_d of the free energy density of the system at temperature T is given by the functional integral

$$\exp\left(-\frac{Af_d}{k_BT}\right) = \prod_x \int_{-d/2}^{+d/2} d\varphi(x)\exp\left(-\frac{E}{k_BT}\right). \qquad (5)$$

The pressure is then obtained as

$$p = -\frac{\partial f_d}{\partial d} \qquad (6)$$

and has the form (2) [1,3]. Our goal is to find the numerical value of the constant α.

Following an idea introduced in Ref. [6] and utilized also in Refs. [7,8], we implement the restriction $-d/2 < \varphi < d/2$ by adding a potential term $m^4 d^2 \int d^2 x V(\varphi/d)$ to E, where V is an even function that is analytic inside a circle with radius $1/2$ and has sufficiently strong singularities at $\pm 1/2$. We then expand the potential V in a Taylor series in φ and drop the restriction on φ. At the end of the calculation, we let $m \to 0$ to recover the hard-wall limit.

Since the functional form of p in terms of κ, d, and T is known and since we differentiate f_d only with respect to d, we set $k_BT = \kappa = 1$ in the sequel. The energy functional may then be written as

$$E = \int d^2 x \left(\frac{1}{2}[\partial^2 \varphi(x)]^2 + \frac{1}{2}m^4 \varphi(x)^2 + m^4 \epsilon_0 d^2 \right.$$
$$\left. + m^4 \sum_{k=2}^{\infty} \epsilon_{2k} d^{2(1-k)} \varphi(x)^{2k} \right), \qquad (7)$$

where the ϵ_{2k} are the expansion coefficients of the potential V.

The above procedure defines a finite-m version $f_d(m)$ of the free energy density f_d of (5), such that $f_d = \lim_{m\to 0} f_d(m)$. $f_d(m)$ may be expanded in a perturbative series in terms of vacuum diagrams—i.e., Feynman diagrams without external legs [6–8]. The technical details of this procedure are described in Ref. [8], and deviations from the treatment in Ref. [8] are delegated to the Appendix. The result is that an expansion of $f_d(m)$ through L loops has the form

$$f_d(m) \approx \frac{1}{d^2} \sum_{l=0}^{L} a_l g^{l-2}, \qquad (8)$$

with the expansion parameter

$$g = \frac{1}{m^2 d^2}. \qquad (9)$$

The perturbative coefficients a_l are functions of the ϵ_{2k}. Combining (2), (6), and (8), we obtain a finite-g version $\alpha(g)$ of α such that an expansion of $\alpha(g)$ through L loops has the form

$$\alpha(g) \approx \frac{1}{4g^2} \sum_{l=0}^{L} a_l g^l, \qquad (10)$$

of which we need to extract the limit

$$\alpha = \lim_{g\to\infty} \alpha(g). \qquad (11)$$

In Secs. IV and V, we consider several resummation schemes for extracting the value of α from a limited number of coefficients a_l.

III. QM PARTICLE IN A BOX

A one-dimensional problem similar to the two-dimensional case above is finding the ground state energy of a QM particle in a one-dimensional box [6,10] (which, in turn, is equivalent to finding the classical partition function of a string with tension between one-dimensional walls [6,10,11]). Introduction of a potential to model the hard walls leads to a quantity $\alpha(g)$ parametrizing the ground state energy of a particle moving in this potential (see Refs. [6,8,10] and the Appendix for details; our notation follows [8]). This quantity has a loop expansion of the form (10) and due to the trivial topologies of the Feynman diagrams through two loops, the coefficients a_0, a_1, and a_2 are identical to those of the membrane case.

For the particular potential

$$V_c(z) = \frac{1}{2\pi^2 \cos^2(\pi z)}, \qquad (12)$$

the exact ground state energy is known (see, e.g., Ref. [10]) and translates into

$$\alpha(g) = \frac{\pi^2}{128}\left(\frac{16}{\pi^4 g^2} + \frac{1}{2} + \frac{4}{\pi^2 g}\sqrt{1 + \frac{\pi^4 g^2}{64}} \right), \qquad (13)$$

giving the limit

$$\alpha = \frac{\pi^2}{128} = 0.077\,106\,284\,38\ldots \qquad (14)$$

for $g \to \infty$. The QM result (13) will be utilized by the resummation schemes of Sec. V to extract α for the membrane problem.

In the sequel, we will always contrast the membrane results with those for the QM problem for the same resummation scheme.

IV. α FROM DIRECT RESUMMATION OF $\alpha(g)$

Knowing only a few low-order coefficients a_l, we are looking for the $g \to \infty$ limit of the series (10). This limit corresponds physically to removing the regulator that suppresses fluctuations in the infrared. In the context of critical phenomena, such series have been successfully resummed using Kleinert's variational perturbation theory (VPT; see Refs. [12–14] and Chaps. 5 and 19 of Refs. [15,16], respectively; improving perturbation theory by a variational principle goes back at least to [17]). Accurate critical exponents

TABLE I. Expansion coefficients for the potential V_c and for a potential V_{mb} that gives the QM coefficients a_l also for the membrane problem.

	V_c	V_{mb}
ϵ_0	$1/(2\pi^2)=0.0506606$	Same
ϵ_2	$1/2=0.5$	Same
ϵ_4	$\pi^2/3=3.28987$	Same
ϵ_6	$17\pi^4/90=18.3995$	18.0284
ϵ_8	$31\pi^6/315=94.6129$	89.5702
ϵ_{10}	$691\pi^8/14175=462.545$	419.568
ϵ_{12}	$10922\pi^{10}/467775=2186.57$	1890.91

[13,14,16] and amplitude ratios [18] have been obtained using VPT.

In this section, we present the results of applying VPT directly to the series (10) as described in Ref. [7] and in Sec. IV of Ref. [8]. We refer the reader to Ref. [8] for the details and just mention that we only present the results of the $q=1$ version of VPT, since the results for self-consistent determination of q from the series (10) remain too imprecise even at the six-loop level.

For the potential (12), which also plays an important role in the resummation variants considered in the sections below, the ϵ_{2k} are listed in Table I, and the corresponding perturbative coefficients a_l are listed for both the QM and the membrane problem in Table II. The membrane's coefficients start deviating from the QM coefficients at the three-loop level. At the beginning, the deviation from the particular feature of the QM series that even loop orders beyond two loops have zero coefficients is small. This gives the membrane's series a structure that can be expected to be in a transitional phase towards its high-order behavior. However, for the VPT resummation scheme to work well and give trustworthy results, it is important that the truncated series to be resummed resembles already the behavior at high orders. Consequently, the dependence on the variational parameter in VPT, when applied directly to the series (10), does not develop increasingly flatter plateaus through the orders considered. Such plateaus are, however, an internal consistency check of the method, and we therefore develop other resummation variants for obtaining α in the sections below. Nevertheless, we provide in Table III the extension to six loops of Eq. (24) in

TABLE II. Perturbative expansion coefficients for both the QM and the membrane problem for the potential V_c.

	QM	Membrane
a_0	$1/2\pi^2=0.0506606$	Same
a_1	$1/8=0.1250000$	Same
a_2	$\pi^2/64=0.1542126$	Same
a_3	$\pi^4/1024=0.0951261$	0.105998
a_4	0	0.026569
a_5	$-\pi^8/262144=-0.0361959$	-0.034229
a_6	0	$-0.083246(13)$

TABLE III. α from VPT as applied in Sec. IV for both the QM and the membrane problem. α_{mb} for $L=2$, 3, 4 and $L=5$ were already obtained in Refs. [7,8], respectively.

L	α_{qm}	α_{mb}
2	0.0385531	0.0385531
3	0.0719411	0.0737974
4	0.0758821	0.0794726
5	0.0767518	0.0813538
6	0.0769910	0.0820175

Ref. [8] for the potential V_c and for comparison also list the corresponding QM results, taken from Table I in Ref. [8]. The results are also plotted in Fig. 1 (dotted-dashed lines), and in spite of the above critical remarks they agree perfectly well with the results of the more refined resummation variants to be discussed below.

In Ref. [19], an attempt was made to extract α from the a_l through six loops using so-called factor and root approximants. However, the achieved accuracy was not high enough for any decision about a discrepancy with the Monte Carlo results (3) and (4).

V. α FROM ZERO OF POTENTIAL

Instead of resumming (10) directly, we apply here the strategy of Sec. VI of Ref. [8]. That is, as a first step we fix the ϵ_{2k} in (7) order by order such that the expansion of $\alpha(g)$ for the membrane problem V_{mb} is identical to that of the QM case with a potential V_c. The resulting ϵ_{2k} are listed in Table I. The second step is then to ask where the resulting potential $V_{mb}(z)$ has the singularities $\pm z_0$ closest to the origin on the real axis. The scaling relation $f \propto 1/d^2$ when $m^2=0$ allows us then to recover α for the membrane case through

$$\alpha_{mb} = 4z_0^2 \alpha_{qm}, \tag{15}$$

with α_{qm} from (14). Since the nearest singularities of V_c are of quadratic type, we may assume that the resulting mem-
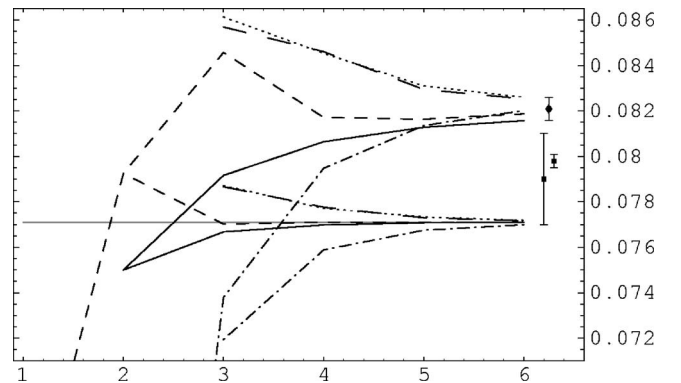

FIG. 1. α_{qm} (lower lines) and α_{mb} (upper lines) as a function of the number of loops L. The horizontal line is the exact QM result. The dotted-dashed, short-dashed, solid, long-dashed, and dotted lines represent data from Tables III, V, VII, VIII, and IX, respectively. Further explanations are given in the main text. At the right, the Monte Carlo results (3) and (4) (boxes) as well as our final result (27) (diamond) are displayed.

TABLE IV. Expansion coefficients of (16) for the quantities $1/\sqrt{V_c}$ and $1/\sqrt{V_{mb}}$.

	QM	Membrane
v_0	$\sqrt{2}\pi = 4.44288$	Same
v_2	$-\pi^3/\sqrt{2} = -21.9247$	Same
v_4	$\pi^5/12\sqrt{2} = 18.0324$	Same
v_6	$-\pi^7/360\sqrt{2} = -5.93242$	10.3394
v_8	$\pi^9/20160\sqrt{2} = 1.04555$	-18.7293
v_{10}	$-\pi^{11}/1814400\sqrt{2} = -0.114657$	-2.24970
v_{12}	$\pi^{13}/239500800\sqrt{2} = 0.00857287$	25.4600

brane potential V_{mb} has approximately such a behavior. We may therefore assume that $1/\sqrt{V_{mb}}$ has approximate linear behavior at its first zero—i.e., at $\pm z_0$.

The simplest investigation of z_0 is to truncate the expansion of $1/\sqrt{V}$ at L loops,

$$1/\sqrt{V(z)} \approx \sum_{l=0}^{L} v_{2l} z^{2l}, \qquad (16)$$

and subsequently numerically determine the first zero of the right-hand side of (16). The v_{2l} for the QM and membrane cases are listed in Table IV. The resulting values of α may be found in Table V. While the correct QM value (14) is approached exponentially fast, the convergence in the membrane case is also remarkable. The results are plotted as short-dashed lines in Fig. 1.

We interpret the fact that the last two differences among the membrane values are comparable as a signal that the maximum achievable accuracy with the current method has been reached. A more refined approach is then needed to take into account a likely more complicated analytic structure of the potential V_{mb}. Let us therefore employ VPT to improve the naive resummation above. Consider the quantity $\sqrt{V(z)} - \sqrt{V(0)}$. At least in QM, the singularities of this quantity nearest to the origin are simple poles. The resulting series

$$F(z) \equiv \sqrt{V(z)} - \sqrt{V(0)} = \sum_{l=1}^{\infty} f_{2l} z^{2l} \qquad (17)$$

may then be inverted to

TABLE V. Results for α for both the QM and the membrane problem using the simple resummation scheme from the beginning of Sec. V.

L	α_{qm}	α_{mb}
1	0.0625000000	Same
2	0.0792468245	Same
3	0.0770188844	0.0845718
4	0.0771087134	0.0817113
5	0.0771062388	0.0816335
6	0.0771062850	0.0818696(2)

TABLE VI. Expansion coefficients of (18) for both the QM and the membrane problem.

	QM	Membrane
u_1	$2\sqrt{2}/\pi = 0.900316$	Same
u_2	$-10/3 = -3.33333$	Same
u_3	$128\sqrt{2}\pi/45 = 12.6375$	13.1791
u_4	$-104\pi^2/21 = -48.878$	-54.6843
u_5	$6904\sqrt{2}\pi^3/1575 = 192.214$	235.065
u_6	$-81784\pi^4/10395 = -766.379$	-1037.10

$$z^2 = \sum_{l=1}^{\infty} u_l F^l. \qquad (18)$$

The first few coefficients u_l for both the QM potential V_c and the resulting membrane potential V_{mb} are listed in Table VI. We are interested in finding

$$z_0^2 = \lim_{F \to \infty} z^2(F). \qquad (19)$$

Motivated by the successes of such an ansatz in critical phenomena, we assume that the function F can be expanded around its first singularities $\pm z_0$ as

$$F = \sum_{k=0}^{\infty} \bar{u}_k (z^2 - z_0^2)^{-q/2+k}, \qquad (20)$$

where $q = 2$ for QM. Inversion of (20) gives

$$z^2 = \sum_{m=0}^{\infty} u'_m F^{-2m/q}, \qquad (21)$$

with $z_0^2 = u'_0$. We may either set $q = 2$ as in QM in the hope that the deviation for the membrane case is small, or determine q self-consistently. We use both approaches below.

Now apply VPT [15,16]. In a truncated expansion

$$z^2 \approx \sum_{l=1}^{L} u_l F^l, \qquad (22)$$

we replace

$$F^l \to (tF)^l \left\{ \left(\frac{F}{\hat{F}}\right)^{2/q} + t\left[1 - \left(\frac{F}{\hat{F}}\right)^{2/q}\right] \right\}^{-lq/2}$$

$$= (t\hat{F})^l \left\{ 1 + t\left[\left(\frac{\hat{F}}{F}\right)^{2/q} - 1\right] \right\}^{-lq/2}, \qquad (23)$$

reexpand the resulting expression in t through t^L, set $t = 1$, and then optimize the resulting expression in $\hat{F}$, where optimizing refers to finding appropriate stationary or turning points according to the principle of minimal sensitivity [20]. That is, we replace

TABLE VII. Results for α when the a_l are fixed to be those of the QM problem and $q=2$ is assumed.

L	α_{qm}	α_{mb}
2	0.0750000	0.0750000
3	0.0766754	0.0791616
4	0.0769828	0.0806435
5	0.0770794	0.0812768
6	0.0770973	0.0815743

$$F^l \to \hat{F}^l \sum_{k=0}^{L-l} \binom{-lq/2}{k} \left[\left(\frac{\hat{F}}{F} \right)^{2/q} - 1 \right]^k \quad (24)$$

and optimize the resulting expression in $\hat{F}$. In the limit $F \to \infty$ of interest to us, this amounts to

$$z_0^2 \approx \mathrm{opt}_{\hat{F}} \left[\sum_{l=1}^{L} u_l \hat{F}^l \sum_{k=0}^{L-l} \binom{-lq/2}{k} (-1)^k \right], \quad (25)$$

which is the L-loop approximation to z_0^2—i.e., using the expansion coefficients through u_L. It turns out that, through the order we are working, there is exactly one extremum for even L and exactly one turning point and no extremum for odd L. This makes the choice of the optimization unique at each order. The value of α is in each case obtained through (15).

The results for $q=2$ are summarized in Table VII and plotted as solid lines in Fig. 1. The correct QM value (14) is approached exponentially fast. The convergence in the membrane case is also remarkable. Though the values are slightly lower than those reported in Tables III and V, they clearly point towards a value of α above the results (3) and (4).

If we refrain from making assumptions about q for $z^2(F)$, we can determine it self-consistently by treating first $d \ln z^2 / d \ln F$ in VPT [13,16], since it has the same q as $z^2(F)$ and since

$$\lim_{F \to \infty} \frac{d \ln z^2}{d \ln F} = 0 \quad (26)$$

by the assumption of a singularity of the potential. That is, we resum the expansion of $d \ln z^2 / d \ln F$ as detailed above and tune q such that optimization with respect to $\hat{F}$ leads to (26). Through two loops, the expansion of $d \ln z^2 / d \ln F$ is q-independent, and we start with $L=3$. It turns out that through the order we are working, we must use turning points for even L and maxima for odd L when determining q. For subsequently determining z_0^2, the situation is reverse—namely, as above for $q=2$.

The results for q and α through six loops are listed in Table VIII. The results for α are plotted as long-dashed lines in Fig. 1. Note how q approaches 2 rapidly for the QM problem and that also for the membrane problem a value around 2 appears to be approached.

An alternative to using (26) for the determination of q is to tune q such that the plateaus at which the result depends least on variations of $\hat{F}$ are optimized [21]. This strategy has

TABLE VIII. Results for q and α when the a_l are fixed to be those of the QM problem and q is determined from its own re-summed series.

L	q_{qm}	α_{qm}	q_{mb}	α_{mb}
3	2.09487	0.0786643	2.26290	0.0856888
4	2.05356	0.0777648	2.21951	0.0846057
5	2.02049	0.0772965	2.11817	0.0829441
6	2.00822	0.0771659	2.08666(1)	0.0825299(2)

been successfully applied in Refs. [21,22] in the context of critical phenomena. In practice, this means finding $\hat{F}$ and q such that first and second derivatives of the right-hand side of (25) with respect to $\hat{F}$ vanish (for turning points) or such that first and third derivatives with respect to $\hat{F}$ vanish (for extrema).

The results for q and α through six loops are listed in Table IX and are very similar to those of Table VIII. They are plotted as dotted lines in Fig. 1.

VI. SUMMARY AND DISCUSSION

In summary, we have computed the constant α parametrizing the pressure law (2) of an infinitely extended fluid membrane between two parallel hard walls. The hard wall was replaced by a smooth potential, allowing for a perturbative loop expansion for α. Several resummation schemes were used to extract the hard-wall limit from expansion coefficients through six loops with results listed in Tables III, V, and VII–IX and plotted in Fig. 1.

The values from Table VII on the one hand and Tables VIII and IX on the other hand approach each other with increasing numbers of loops from below and above, respectively. A conservative procedure for combining our results for α is to average the lowest and highest six-loop values for α obtained above (i.e., the values for α from Tables VII and IX, respectively) and take their difference to be the full error bar. This provides our final result

$$\alpha = 0.0821 \pm 0.0005, \quad (27)$$

displayed in Fig. 1. It lies above the Monte Carlo results (3) and (4), also displayed in Fig. 1. The simplest explanation we have to offer for this discrepancy is that their error bars, in particular that of (4), may have been chosen too optimistic. Also, finite-size or other systematic effects may not have been taken into account properly.

TABLE IX. Results for q and α when the a_l are fixed to be those of the QM problem and q is determined from optimized plateaus.

L	q_{qm}	α_{qm}	q_{mb}	α_{mb}
3	2.09730	0.0787132	2.28225	0.0861317
4	2.04990	0.0777101	2.21532	0.0845332
5	2.02405	0.0773337	2.13061	0.0830987
6	2.00948	0.0771767	2.09303(1)	0.0825984(2)

TABLE X. Numbers of diagrams for low loop orders.

Number of loops l	0	1	2	3	4	5	6	7
Diagrams	1	1	1	3	7	24	83	376
Diags. after one-loop resummation	1	1	1	2	3	11	29	125
Diags. with l-loop topology	1	1	0	1	1	5	8	37

On the other hand, it is possible that the treatment in our work is inflicted by systematic errors. Experience with VPT tells that the internal consistency checks, especially the development of increasingly flatter plateaus in the optimization procedure with higher orders, are reliable indicators of VPT to work. These checks have successfully been implemented for the procedures of Sec. V. Nevertheless, it cannot be ruled out that the method used here is not flexible enough to adequately take into account the unknown true analytical structure of $\alpha(g)$.

Another concern is the value of q_{mb}. While the treatments leading to the α values listed in Tables VIII and IX and thus leading to the upper dotted and long-dashed curves in Fig. 1 determine q_{mb} self-consistently, the QM-inspired value $q_{\mathrm{mb}}=2$ was somewhat arbitrarily chosen to obtain the values for α in Table VII. What if the value of q_{mb} describing $\alpha(g)$ best differs from 2? A slightly larger value (but below the ones from the self-consistent determinations of q_{mb}) leads to slightly increased values of α and therefore also to a larger mean value and smaller error bar in (27). On the other hand, a slightly smaller value leads to slightly decreased values of α and therefore also to a smaller mean value and larger error bar in (27). In both cases, the $q_{\mathrm{mb}}=2$ curve may still approach the correct result. For an optimal value of q_{mb} below 2 this may happen by decreasing α values at higher orders (that such a behavior is possible in principle is easily tested by setting q_{mb} to a value above 2.085, which causes the corresponding six-loop value for α to drop below that at five loops). The smooth behavior and slow flattening of the $q_{\mathrm{mb}}=2$ curve lets us believe, though, that such a drop, if present, should be very small. The best q_{mb} value can thus be expected to lie at most slightly below 2, leading to only a small decrease of the values of Table VII and the upper solid curve in Fig. 1 and to a slightly lower mean value and larger error bar than given in (27). It is reassuring that the results of both the direct resummation of $\alpha(g)$ employed in Sec. IV and the naive resummation from the beginning of Sec. V lie very close to the mean value of (27).

All things considered, we are rather confident about our result (27), but further studies of the system are required to settle the question of the correct value of α.

APPENDIX: FEYNMAN DIAGRAMS

In Ref. [8], we have described at length how recursion relations along the lines of Refs. [23–25] can be used to construct the vacuum diagrams needed for the computation of the perturbative coefficients a_l in (10) through a given loop order, and there is no need to repeat the derivation here. Given the Feynman diagrams, a vertex with $2k$ lines represents a factor

$$-m^4 d^{2(1-k)}\epsilon_{2k}, \tag{A1}$$

and the perturbative coefficients a_l are obtained from the sum of l-loop diagrams as

$$a_l = -\sum_n c_{l-n} g_{l-n} I_{l-n}, \tag{A2}$$

where c_{l-n} is a combinatorial factor, g_{l-n} is a monomial in the ϵ_{2k}, and I_{l-n} is the corresponding momentum space integral. The integration measure is $\int d^D k/(2\pi)^D$ with $D=1$ for QM and $D=2$ for the membrane. The membrane propagator carrying a momentum $\mathbf{k}$ is given by $1/(k^4+m^4)$, while the QM propagator carrying a momentum k is given by $1/(k^2+m^2)$.

From the list of diagrams through five loops in Ref. [8] it is obvious that a major reason for the rapid increase of the number of Feynman diagrams with the number of loops is a proliferation of the momentum-independent one-loop propagator insertions of the form $\bigcirc$. A simple measure to reduce the number of diagrams to be considered is a one-loop resummation where we absorb the above insertion into the parameter m in the propagator and at the end reexpand the resulting modified perturbative series in powers of g as was carried out in Ref. [25] and treated on a more formal level in Ref. [24]. Note that many other resummations in the form of momentum-independent propagator and vertex corrections are possible, leading to a further reduction of the number of Feynman diagrams. However, at the current level of computing vacuum diagrams through six loops, this is unnecessary. In any case, the diagrams most difficult to evaluate are always those with the full loop topology and remain after any such resummation.

To implement the one-loop resummation in the membrane case, we must compute diagrams with a modified propagator H such that

$$G_{12}^{-1} = H_{12}^{-1} - 12 L_{1234}^{(4)} H_{34}, \tag{A3}$$

where the notation of Ref. [8] has been employed. Writing $G^{-1}=k^4+m^4$ and $H^{-1}=k^4+M^4$, this condition translates into

$$k^4 + m^4 = k^4 + M^4 - \tfrac{3}{2}m^4 d^{-2}\epsilon_4 M^{-2} \tag{A4}$$

or

$$\left(\frac{M^2}{m^2}\right)^3 - \left(\frac{M^2}{m^2}\right) - \frac{3}{2}\epsilon_4 g = 0, \tag{A5}$$

where we have used (9) and the one-loop result

$$\int \frac{d^2 k}{(2\pi)^2} \frac{1}{k^4+m^4} = \frac{1}{8m^2}. \tag{A6}$$

Define $Z(g)$ by

TABLE XI. Diagrams l-n (nth l-loop diagram) through six loops, their combinatorial factors c_{l-n}, coupling constant factors g_{l-n}, and values I_{l-n} of the corresponding integrals for $M=1$. $D=1$ and $D=2$ correspond to the QM and membrane problems, respectively.

l–n	diagram	c_{l-n}	g_{l-n}	$I^{D=1}_{l-n}$	$I^{D=2}_{l-n}$
0-1	•	1	$-\epsilon_0$	1	1
1-1		$\dfrac{1}{2}$	1	-1	$-\dfrac{1}{4}$
2-1		-3	$-\epsilon_4$	$\dfrac{1}{4}$	$\dfrac{1}{64}$
3-1		12	ϵ_4^2	$\dfrac{1}{32}$	4.04576×10^{-4}
3-2		15	$-\epsilon_6$	$\dfrac{1}{8}$	$\dfrac{1}{512}$
4-1		288	$-\epsilon_4^3$	$\dfrac{3}{512}$	1.63237×10^{-5}
4-2		360	$\epsilon_4\epsilon_6$	$\dfrac{1}{64}$	5.05719×10^{-5}
4-3		105	$-\epsilon_8$	$\dfrac{1}{16}$	$\dfrac{1}{4096}$
5-1		2592	ϵ_4^4	$\dfrac{5}{4096}$	7.55133×10^{-7}
5-2		2304	ϵ_4^4	$\dfrac{19}{12288}$	1.04187×10^{-6}
5-3		10368	ϵ_4^4	$\dfrac{7}{6144}$	6.71540×10^{-7}
5-4		5760	$-\epsilon_4^2\epsilon_6$	$\dfrac{7}{3072}$	1.50770×10^{-6}
5-5		12960	$-\epsilon_4^2\epsilon_6$	$\dfrac{3}{1024}$	2.04047×10^{-6}
5-6		4320	$-\epsilon_4^2\epsilon_6$	$\dfrac{5}{1024}$	3.95093×10^{-6}
5-7		360	ϵ_6^2	$\dfrac{1}{192}$	3.76084×10^{-6}
5-8		2700	ϵ_6^2	$\dfrac{1}{128}$	6.32149×10^{-6}
5-9		2025	ϵ_6^2	$\dfrac{1}{64}$	$\dfrac{1}{65536}$
5-10		5040	$\epsilon_4\epsilon_8$	$\dfrac{1}{128}$	6.32149×10^{-6}
5-11		945	$-\epsilon_{10}$	$\dfrac{1}{32}$	$\dfrac{1}{32768}$
6-1		$\dfrac{124416}{5}$	$-\epsilon_4^5$	$\dfrac{35}{131072}$	3.74650×10^{-8}
6-2		248832	$-\epsilon_4^5$	$\dfrac{71}{294912}$	3.12644×10^{-8}
6-3		165888	$-\epsilon_4^5$	$\dfrac{367}{1179648}$	4.52023×10^{-8}
6-4		497664	$-\epsilon_4^5$	$\dfrac{269}{1179648}$	2.85447×10^{-8}
6-5		$\dfrac{331776}{5}$	$-\epsilon_4^5$	$\dfrac{5}{24576}$	$2.37861(5) \times 10^{-8}$
6-6		27648	$-\epsilon_4^5$	$\dfrac{25}{65536}$	6.39380×10^{-8}
6-7		414720	$\epsilon_4^3\epsilon_6$	$\dfrac{65}{147456}$	6.27924×10^{-8}
6-8		207360	$\epsilon_4^3\epsilon_6$	$\dfrac{5}{12288}$	5.50218×10^{-8}
6-9		138240	$\epsilon_4^3\epsilon_6$	$\dfrac{19}{24576}$	1.30234×10^{-7}
6-10		155520	$\epsilon_4^3\epsilon_6$	$\dfrac{5}{8192}$	9.43917×10^{-8}
6-11		622080	$\epsilon_4^3\epsilon_6$	$\dfrac{7}{12288}$	8.39425×10^{-8}
6-12		155520	$\epsilon_4^3\epsilon_6$	$\dfrac{1}{1024}$	1.70039×10^{-7}
6-13		34560	$\epsilon_4^3\epsilon_6$	$\dfrac{5}{8192}$	1.02301×10^{-7}
6-14		51840	$\epsilon_4^3\epsilon_6$	$\dfrac{5}{4096}$	2.46933×10^{-7}

TABLE XI. (*Continued.*)

$l-n$	diagram	c_{l-n}	g_{l-n}	$I^{D=1}_{l-n}$	$I^{D=2}_{l-n}$	$l-n$	diagram	c_{l-n}	g_{l-n}	$I^{D=1}_{l-n}$	$I^{D=2}_{l-n}$
6-15		161280	$-\epsilon_4^2\epsilon_8$	$\dfrac{7}{6144}$	1.88463×10^{-7}	6-22		32400	$-\epsilon_4\epsilon_6^2$	$\dfrac{1}{512}$	3.95093×10^{-7}
6-16		181440	$-\epsilon_4^2\epsilon_8$	$\dfrac{3}{2048}$	2.55058×10^{-7}	6-23		129600	$-\epsilon_4\epsilon_6^2$	$\dfrac{5}{2048}$	4.93867×10^{-7}
6-17		20160	$-\epsilon_4^2\epsilon_8$	$\dfrac{1}{1024}$	1.63681×10^{-7}	6-24		24300	$-\epsilon_4\epsilon_6^2$	$\dfrac{1}{256}$	$\dfrac{1}{1048576}$
6-18		40320	$-\epsilon_4^2\epsilon_8$	$\dfrac{5}{2048}$	4.93867×10^{-7}	6-25		75600	$\epsilon_4\epsilon_{10}$	$\dfrac{1}{256}$	7.90187×10^{-7}
6-19		64800	$-\epsilon_4\epsilon_6^2$	$\dfrac{1}{1152}$	1.31735×10^{-7}	6-26		20160	$\epsilon_6\epsilon_8$	$\dfrac{1}{384}$	4.70105×10^{-7}
6-20		172800	$-\epsilon_4\epsilon_6^2$	$\dfrac{7}{6144}$	1.88463×10^{-7}	6-27		75600	$\epsilon_6\epsilon_8$	$\dfrac{1}{256}$	7.90187×10^{-7}
6-21		194400	$-\epsilon_4\epsilon_6^2$	$\dfrac{3}{2048}$	2.55058×10^{-7}	6-28		37800	$\epsilon_6\epsilon_8$	$\dfrac{1}{128}$	$\dfrac{1}{524288}$
						6-29		10395	$-\epsilon_{12}$	$\dfrac{1}{64}$	$\dfrac{1}{262144}$

$$M^2 = Z(g)m^2. \qquad (A7)$$

Although (A5) can be solved analytically for $Z(g)$, it is more useful for our purposes to write

$$Z(g) = 1 + \sum_{k=1}^{\infty} c_k g^k \qquad (A8)$$

and extract

$$c_1 = \tfrac{3}{4}\epsilon_4 \qquad (A9)$$

and the recursion relation

$$c_k = -\frac{3}{2}\sum_{i=1}^{k-1} c_i c_{k-i} - \frac{1}{2}\sum_{i=1}^{k-2}\sum_{j=1}^{k-i} c_{k-i-j}c_i c_j, \quad k > 1. \quad (A10)$$

Through six loops in the vacuum diagrams, we need $Z(g)$ through g^5 and obtain

$$Z(g) = 1 + \tfrac{3}{4}\epsilon_4 g - \tfrac{27}{32}\epsilon_4^2 g^2 + \tfrac{27}{16}\epsilon_4^3 g^3 - \tfrac{8505}{2048}\epsilon_4^4 g^4$$
$$+ \tfrac{729}{64}\epsilon_4^5 g^5 + \mathcal{O}(g^6). \qquad (A11)$$

The same resummation (A3) can be implemented for the QM case. Writing $G^{-1} = k^2 + m^2$ and $H^{-1} = k^2 + M^2$, the condition (A3) translates now into

$$k^2 + m^2 = k^2 + M^2 - 6m^2 d^{-2}\epsilon_4 M^{-1} \qquad (A12)$$

or

$$\left(\frac{M}{m}\right)^3 - \left(\frac{M}{m}\right) - \frac{3}{2}\epsilon_4 g = 0, \qquad (A13)$$

where we have used $g = 4/md^2$ [8] and the one-loop result

$$\int_{-\infty}^{+\infty} \frac{dk}{2\pi}\frac{1}{k^2 + m^2} = \frac{1}{2m}. \qquad (A14)$$

This time we define $Z(g) \equiv M/m$. Then $Z(g)$ is the same as in the membrane case considered above.

The resulting modifications in the Feynman rules are for both the membrane and the QM case:

(1) Discard all vacuum diagrams with one or more one-loop propagator insertions , with the exception of the two-loop diagram, which changes sign (here, the combinatorics do not work out; loosely speaking, it is undefined which part of the diagram is the insertion).

(2) Compute all remaining diagrams with the replacement $m \rightarrow M$ in the propagators.

(3) Replace $M^2 \rightarrow Z(g)m^2$ for the membrane case and $M \rightarrow Z(g)m$ for the QM case and reexpand the perturbative series in powers of g.

In Table X, we give the original numbers of diagrams at some low loop orders, the numbers left after our one-loop resummation, and the numbers of diagrams with the full respective loop topology. The latter is necessarily the same both before and after the one-loop resummation. In Table XI, we list all diagrams through six loops left after the one-loop resummation. Also given are their combinatorial factors c_{l-n}, their coupling constant factors g_{l-n}, and the values I_{l-n} of the corresponding integrals for $M=1$ for both the QM and the membrane problem (the multiplying power of M can immediately be inferred from the number of loops and propagators of a given diagram).

The techniques for evaluating the integrals are explained in Ref. [8]. With the exception of I_{6-5}, the membrane integrals have been evaluated to the precision given either in momentum space or in both momentum and configuration space. For I_{6-5}, the indicated precision could only be obtained in configuration space. Since the slightly lower precision of I_{6-5} introduces the main computational error into the determination of α at the six-loop level, we have indicated the ensuing numerical error in the other tables of this work, where applicable.

---

[1] W. Helfrich, Z. Naturforsch. A **33A**, 305 (1978); W. Helfrich and R. M. Servuss, Nuovo Cimento D **3**, 137 (1984).

[2] I. Bivas and A. G. Petrov, J. Theor. Biol. **88**, 459 (1981); D. Sornette and N. Ostrowsky, J. Phys. (France) **45**, 265 (1984).

[3] W. Janke and H. Kleinert, Phys. Lett. A **117**, 353 (1986).

[4] W. Janke, H. Kleinert, and M. Meinhart, Phys. Lett. B **217**, 525 (1989).

[5] G. Gompper and D. M. Kroll, Europhys. Lett. **9**, 59 (1989).

[6] H. Kleinert, Phys. Lett. A **257**, 269 (1999).

[7] M. Bachmann, H. Kleinert, and A. Pelster, Phys. Lett. A **261**, 127 (1999).

[8] B. Kastening, Phys. Rev. E **66**, 061102 (2002).

[9] W. Janke and H. Kleinert, Phys. Rev. Lett. **58**, 144 (1987); F. David, J. Phys. (France) **51**, C7115 (1990); R. R. Netz and R. Lipowsky, Europhys. Lett. **29**, 345 (1995); M. Bachmann, H. Kleinert, and A. Pelster, Phys. Rev. E **63**, 051709(R) (2001).

[10] H. Kleinert, A. Chervyakov, and B. Hamprecht, Phys. Lett. A **260**, 182 (1999).

[11] P.-G. de Gennes, J. Chem. Phys. **48**, 2257 (1968); R. Lipowsky, Z. Phys. B: Condens. Matter **97**, 193 (1995); C. Hiergeist and R. Lipowsky, Physica A **244**, 164 (1997).

[12] H. Kleinert, Phys. Lett. A **207**, 133 (1995).

[13] H. Kleinert, Phys. Rev. D **57**, 2264 (1998); **58**, 107702 (1998).

[14] H. Kleinert, Phys. Rev. D **60**, 085001 (1999); Phys. Lett. A **277**, 205 (2000).

[15] H. Kleinert, *Path Integrals in Quantum Mechanics, Statistics, Polymer Physics, and Financial Markets*, 3rd ed. (World Scientific, Singapore, 1995), Chap. 5.

[16] H. Kleinert and V. Schulte-Frohlinde, *Critical Properties of ϕ^4-Theories*, 1st ed. (World Scientific, Singapore, 2001), Chap. 19.

[17] V. I. Yukalov, Moscow Univ. Phys. Bull. **31**, 10 (1976).

[18] H. Kleinert and B. Van den Bossche, Phys. Rev. E **63**, 056113 (2001).

[19] V. I. Yukalov and S. Gluzman, Int. J. Mod. Phys. B **18**, 3027 (2004).

[20] P. M. Stevenson, Phys. Rev. D **23**, 2916 (1981).

[21] B. Hamprecht and H. Kleinert, Phys. Rev. D **68**, 065001 (2003).

[22] B. Kastening, Phys. Rev. A **70**, 043621 (2004).

[23] H. Kleinert, A. Pelster, B. Kastening, and M. Bachmann, Phys. Rev. E **62**, 1537 (2000).

[24] B. Kastening, Phys. Rev. E **61**, 3501 (2000).

[25] B. Kastening, Phys. Rev. D **54**, 3965 (1996); **57**, 3567 (1998).